LAWRENCE
LIVERMORE
NATIONAL
LABORATORY

LLNL-JRNL-560176

Determining the Pharmacokinetics and Long-term Biodistribution of SiO2 Nanoparticles in vivo using Accelerator Mass Spectrometry

M. A. Malfatti, H. A. Palko, E. A. Kuhn, K. W. Turteltaub

June 7, 2012

Nano Letters

Disclaimer

DETERMINING THE PHARMACOKINETICS AND LONG-TERM BIODISTRIBUTION OF SiO_2 NANOPARTICLES *IN VIVO* USING ACCELERATOR MASS SPECTROMETRY

Michael A. Malfatti, Heather A. Palko, Edward A. Kuhn, and Kenneth W. Turteltaub

Biosciences and Biotechnology Division, Physical and Life Sciences Directorate
Lawrence Livermore National Laboratory, Livermore, CA
Battelle Center for Fundamental and Applied Systems Toxicology (B-FAST)
Multi-scale Toxicology Initiative, Battelle Memorial Institute, Columbus, OH

Corresponding author:
Michael A. Malfatti, PhD
Biosciences and Biotechnology Division
Lawrence Livermore National Laboratory
7000 East Avenue, L-452
Livermore, CA 94583
Phone: 925-422-5732
Email: malfatti1@llnlgov

Running title: The use of AMS to determine the pharmacokinetics of SiO_2 nanoparticles

Key Words: accelerator mass spectrometry, nanoparticles, pharmacokinetics, biodistribution

ABSTRACT

The ever-increasing use of silica dioxide nanoparticles (SiNPs) for a wide variety of commercial and biomedical applications has led to concerns about their biosafety. As the potential for SiNP exposure increases, the investigation of their biological fate has not kept pace. To understand SiNP biodisposition, it is essential to comprehensively determine the pharmacokinetic (PK) parameters, biodistribution, and elimination kinetics. However, these comprehensive studies are lacking, most likely due to the lack of suitable analytical methods. To investigate the relationship between administered dose, PK, and long-term biodistribution, the ultra-sensitive technique of accelerator mass spectrometry (AMS) was used to determine the PK parameters and tissue distribution of ^{14}C-SiNPs in mice. AMS measures isotope ratios with high selectivity, which allows for the quantification of extremely low concentrations of material with high sensitivity and precision, enabling long-term kinetic studies. Male BALB/c mice were administered a single intravenous dose of ^{14}C-SiNPs, and blood and tissue were collected at specific time points over an 8-week time period. Nanoparticle concentration in blood, tissue, and excreta was determined by quantifying the amount of radiocarbon equivalents in each sample by AMS. Plasma PK analysis showed that the SiNPS were rapidly cleared from the central compartment with a distribution half-life of 0.38 h. The apparent volume of distribution of 2058.1 ml/kg indicated extensive distribution to tissues. AMS analysis revealed that SiNPS were rapidly distributed to the tissues of the reticuloendothelial system including liver, spleen, kidney, lung, and bone marrow, and persisted in the tissue over the 8-week time course of the study. Elimination of SiNPs occurred by both the renal and biliary routes. These results indicate that AMS is an effective tool to accurately and precisely quantify the long-term kinetics and biodistribution of SiNPs *in vivo*.

INTRODUCTION

The ever-increasing use of nanoparticles (NPs) for a wide variety of commercial, industrial, and biomedical applications has led to concerns about their biosafety. Because of their unique properties such as monodispersity, large surface area, and high drug loading efficiency [1, 2], silica nanoparticles (SiNPS) have been developed for a vast array of biomedical uses such as optical imaging [3], cancer therapy [4], targeted drug delivery [5] and controlled drug release for genes and proteins [6, 7]. Silica nanoparticles are also found in many personal care products and in certain foods [8]. However, as the potential uses of SiNPs have increased at a rapid rate, the evaluation of their biological fate and toxicity has not kept pace[9]. Currently, a complete understanding of the size, shape and composition-dependent interactions of SiNPs with biological systems is lacking [10], and thus it is unclear whether these particles can elicit a toxic biological response [11]. Therefore, a systematic and thorough quantitative analysis of the absorption, distribution, elimination, and pharmacokinetics (PK) is needed for a better understanding of SiNP interactions with tissues and cell types, and for assessments of basic distribution and clearance that serve as the basis in determining toxicity.

Previous studies have shown that the inhalation of microscale silica is potentially linked with the pulmonary disease silicosis in humans [11]. Chronic inhalation studies in rats have been associated with pulmonary fibrosis and cancer [12]. It is likely that the unique properties of SiNPs may impose different biological effects than what has been reported from microscale particles. Thus, the biological fate of SiNPs warrant further investigation. In contrast to a significant number of studies that have reported on the biological fate of other nanoparticles such as quantum dots [13, 14], liposomes [15, 16], and carbon nanotubes [17, 18], studies on the biodistribution and PK of SiNPs are lacking. This is likely due to the lack of suitable analytical methods.

Most studies to date that have investigated *in vivo* biodistribution of SiNPs have relied on fluorescence detection techniques and have been qualitative in nature [19-22]. In all these studies, results showed that SiNPs distributed primarily to the liver and spleen. Cho *et al*. showed that SiNPs, when administered to mice

intravenously (IV), induced an inflammatory response in the liver and were retained in both the liver and spleen up to 4 weeks after dosing [19]. Likewise, He *et al.* reported, using fluorescence intensity measurements, that mesoporous silica distribute mainly to the liver and spleen with small quantities being found in the lung, kidney, and heart. Furthermore, in a study using ^{125}I-labeled SiNPs, Xie *et al.* reported that SiNPs administered IV to mice accumulate mainly in the lungs, liver, and spleen and are retained for 30 days in the tissue. As these studies contribute to the understanding of SiNP biodistribution and show that SiNPs distribute mainly to tissues of the reticuloendothelial system, comprehensive, quantitative long-term biodistribution and pharmacokinetic studies are still needed to better understand the relationship between administered dose, biological fate and ultimate toxicity.

To investigate the PK properties and the quantitative long-term tissue distribution of SiNPs, the ultra sensitive technique of Accelerator Mass Spectrometry (AMS) was used to determine the PK parameters and biological fate of ^{14}C-SiNPs in mice. AMS is a technique for the measurement of rare, long-lived isotopes with extremely high sensitivity. AMS counts isotopes independent of radioactive decay by measuring the mass ratio of the radioisotope of interest relative to a stable isotope of the element. AMS can be used to trace the fate of any molecule in *in vitro* systems or whole organisms if it is labeled with an isotope appropriate for AMS analysis. Because most biological materials contain carbon, the majority of biological AMS studies use ^{14}C as the radiotracer. AMS can detect and quantify a ^{14}C-labeled compound in a biological matrix with 1%-3% precision at levels ranging from approximately 10 pmol ^{14}C to 1 attomol (1×10^{-18}) ^{14}C in samples containing 1 mg of total carbon[23, 24]. Studies with AMS in laboratory animals to determine the kinetics of absorption, distribution, and excretion, and to identify and quantify metabolites using chemical doses of 0.1 to 500 ng/kg body weight and radioisotope doses of under 10 nCi/kg can be routinely carried out [25, 26]. The sensitivity of AMS measurement gives this technique a number of major advantages over other methods for the detection of isotopes. Importantly, because of the extreme sensitivity, PK studies have the ability to determine long-term kinetics and metabolism using low doses for several months after isotope

administration. Furthermore, since only low doses of chemical and radioactivity are required, studies can be performed with levels of chemicals equivalent to therapeutic or environmental exposures. This is a significant feature because the biological effects observed at high doses may not extrapolate to the low doses that are typically encountered in real exposure scenarios. In addition, detailed pharmacokinetic data require frequent sampling, which is made possible with AMS detection, by virtue of the small sample sizes needed for analysis. AMS has been used to establish the kinetics of β-carotene uptake and plasma clearance in a human volunteer who received a single dose of ^{14}C-β-carotene obtained from ^{14}C labeled spinach [27]. Plasma concentrations of β-carotene and its metabolites were determined at intervals over a 7-month period and required just 30 μl of plasma/analysis. Such complete investigations would not be possible using other methods that lack the necessary sensitivity to detect compounds and metabolites months after dosing.

To assess the suitability of AMS as a technique to evaluate the PK and long-term tissue distribution of SiNPs, mice were dosed (IV) with a single injection of ^{14}C-SiNPs and blood and tissues were collected at specified time intervals during an 8 week period after SiNP administration. Nanoparticle concentration in blood and tissue was determined by quantifying the amount of ^{14}C radiolabel in the samples by AMS. Results from the current study show plasma concentration curves from mice dosed with the ^{14}C-SiNPs to have a rapid plasma clearance and are distributed primarily to tissues of the reticuloendothelial system. Particles remained in the tissues throughout the 8-week duration of the study, while a percentage was excreted in both the urine and feces. These results indicate that AMS is an effective tool to accurately and precisely quantify the PK properties and long-term biodistribution of SiO_2 nanoparticles *in vivo*.

RESULTS AND DISCUSSION

This is the first study to use AMS to quantitatively track nanoparticles *in vivo*. Because of the extreme sensitivity and precision of AMS, it was possible to track the

SiNPs out to 8 weeks post exposure. The decision to end the study at 8 weeks was arbitrary, and was not limited due to the detection limits of AMS. In fact, the results indicate that AMS is capable of detecting the SiNPs for longer exposure times, perhaps up to several months after exposure. This study was also the first to use AMS to measure a nonsoluble test article. The SiNPS used in the study do not breakdown and do not solubilize in a biological matrix. Because of this, tissue homogenization methods were developed to ensure there was a uniform sampling distribution of SiNPS within each tissue that was analyzed. To test the efficiency of the homogenization process, SiNP concentration in homogenized liver and spleen samples from mice exposed to ^{14}C-SiNPs were compared to whole un-homogenized liver and spleen with the same treatment. For both liver and spleen the mean tissue concentrations of SiNPs were similar for the whole tissue samples and the homogenate samples. However, homogenization of the tissue resulted in less variation in sample-to-sample measurements compared to measurements in whole tissues. Therefore, all subsequent analyses employed the tissue homogenization procedure prior to AMS analysis.

The use of AMS allowed for the precise quantification and comprehensive assessment of the plasma PK parameters of SiNPs. Figure 1 depicts the plasma ^{14}C-SiNP concentration versus time data over 48 h following intravenous administration of ^{14}C-SiNP in mice. Based on ^{14}C equivalents, the SiNPS were rapidly cleared from the central compartment following first order processes with a mean distribution half-life ($t_{1/2}\alpha$) of 0.38 h and an elimination half-life ($t_{1/2}\beta$) of 78.4 h (Table 1). The obtained $t_{1/2}\alpha$ is consistent to what was reported for paramagnetic quantum dot containing silica nanoparticles of similar size [28]. The long $t_{1/2}\beta$ indicates that not all the nanoparticles were cleared from the plasma within the 48 h sampling time. This is consistent with the measurements taken over the 8-week exposure time revealing appreciable levels of SiNPS in the plasma over the study period. These findings indicate that a portion of the dose remains in the plasma over an extended period of time, perhaps due to recirculation of SiNPS through enterohepatic circulation, or a delayed release of SiNPS from extrahepatic tissue back into the blood stream,

resulting in a fraction of the dose having a long residence time.

The calculated mean pharmacokinetic parameters are presented in Table 1. Initial plasma concentration ($C_{initial}$) of ^{14}C-SiNPs was determined to be 154.0 µg/ml, and the mean plasma clearance rate (Cl) was calculated to be 18.2 ml/hr /kg. The apparent volume of distribution (V_d) was 2058.1 ml/kg. These values indicate a rapid and extensive distribution beyond the central compartment, which implies SiNPs must accumulate in organ tissues. The mean $AUC_{(0-t)}$ value was 445.5 µg-hr/ml, whereas the mean $AUC_{(0-\infty)}$ was 1099.4 µg-hr/ml. The greater than 2-fold increase in $AUC_{(0-\infty)}$ compared to $AUC_{(0-t)}$ is consistent with the long $t_{1/2}\beta$ indicating there was a significant level of nanoparticles remaining is the plasma beyond the 48 h sampling time. Applying a 2-compartment open model, the absorption rate of nanoparticles to the peripheral compartment from the central compartment (k_{12}) was 1.57 hr^{-1}. The k_{21} rate constant (transfer rate of nanoparticles from the peripheral compartment to the central compartment) was 0.11 hr^{-1}, and the elimination rate constant (k_{10}) was 0.14 hr^{-1}. The higher k_{12} compared to the k_{21} and k_{10} re-enforce the concept that the majority of the SiNP dose is rapidly eliminated from the plasma and distributed to tissues.

The extreme sensitivity afforded by AMS allowed for the quantitative tissue distribution of SiNPs to be evaluated over an 8-week time course. Initial concentrations of SiNPs in tissue were assessed at time points of 0.25, 0.5, 1.0, 2.0, 8.0 and 24 hours after SiNP administration. Long-term distribution was determined at 1, 2, 7, 14, 28, 42 and 56 days post SiNP dosing. The results are reported as µg nanoparticles/gram of tissue in Table 2. For clarity of the initial distribution, graphical representation of SiNP tissue concentration for liver, spleen, kidney, lung, and cervical lymph nodes, over the first 24 h sampling time is depicted in Figure 2. After IV administration, initial biodistribution of SiNPs was rapid and was confined primarily to tissues of the reticuloendothelial system including the spleen, liver, kidney, lung, and cervical lymph nodes. There were also appreciable amounts detected in the bone marrow. The more peripheral tissue had much less accumulation of SiNPs. There was little or no distribution of SiNPs to the brain,

muscle or adipose tissue. This is most likely due to the inability of the SiNPS to cross the blood brain barrier and the low blood perfusion rate in the striated muscle and adipose tissue, compared to the highly perfused organ tissues. Quantitative analysis revealed that the concentrations of SiNPS varied from tissue to tissue with the highest concentrations occurring in the spleen and liver, followed by lung and kidney. In all tissues examined, the Cmax concentration of SiNPs occurred within 2 h after dosing indicating a rapid distribution to the tissues. The spleen had the highest mean concentration of SiNPs at 298.6 μg/gm at 2 hr post dose followed by the liver, kidney, and cervical lymph nodes at 228.2 μg/gm and 56.91 μg/gm, and 33.9 μg/gm, respectively (Figure 2). The overall amounts of SiNPS were actually higher in the liver when compared to the spleen, although their biodistribution densities were lower due to the size differential of the liver to that of the spleen. When adjusted to total tissue weight, at 2 h post dose, the liver contained the highest proportion of the dose at an average of 62% of the administered dose followed by the spleen, kidney and lung at 6.4%, 5.1%, and 1.5%, respectively. All other tissues contained less than 1% of the administered dose. These results are consistent with a previous study by Xie *et al*. who reported that both 20 nm and 80 nm SiNPs primarily accumulated in the spleen, liver, and lung, after a single IV dose of ^{125}I-SiNPs [9]. Several other studies using qualitative techniques to detect SiNPs of various sizes confirm the results from this current study showing SiNPs accumulate primarily in the liver, spleen lung and bone marrow [19-21, 28]. In these studies the SiNPs were located primarily in the phagocytic cells in the liver, spleen, and bone marrow. In the lung, accumulation was primarily due to entrapment of the particles in the pulmonary vasculature.

The rate of change in SiNP concentration over time varied between tissues. In the liver, spleen, kidney, and lung, between 2-24 hr, the decrease in SiNP concentration ranged between 67-72%. In the cervical lymph nodes the concentration decreased by over 82% over the same time period. The bone marrow had the largest decrease in SiNP concentration of 87% from 0.25 h to 24 hr. The large decrease in the lymph tissue and bone marrow is consistent with the rapid elimination of the SiNPS from the plasma. The concentrations of SiNPs within each

tissue were also ever changing with time after administration. This could be attributed to the different capture rates of the various tissues and the level of circulating SiNPS in the blood and lymph.

Long-term biodistribution revealed that the overall trend was a gradual decline in SiNP levels over time (Table 2). However, there was a significant amount of SiNPS remaining in the tissues 8 weeks after administration. In the kidney and lung, between 1 and 56 days after SiNP exposure, there was only a 20% decrease in SiNP concentration. In the liver and spleen there was a 72% and 57% decline in SiNP concentration, respectively, over the same time period (Table 2). In the lung, at 7 days post exposure the concentration of particles increased by 68% over the two-day concentration level and remained elevated through 14 days. In the spleen there was a similar increase between 14 and 28 days. The persistence of SiNPS in the tissues is most likely attributed to the uptake by macrophages residing within these tissues that are involved in the capture and metabolism of foreign particles and molecules [9, 29]. Furthermore, the finding of SiNPs in the cervical lymph nodes and bone marrow, and their presence for up to 8 weeks suggest that there is the potential for an immune response from exposure to these SiNPs. In a similar study, Cho *et al*. showed that 50, 100 and 200 nm-sized SiNPs, when administered to mice IV, induced an inflammatory response in the liver and were retained in both the liver and spleen up to 4 weeks after dosing [19].

Clearance of the SiNPs occurred through both the renal and biliary elimination routes (Figure 3). Of the total amount of SiNP excreted over the first 24 h of the study duration 69.4% was eliminated in the urine, whereas, 30.6% was found in the feces. In the urine the Cmax of 62.4 μg/ml occurred 2 hr post dose administration (Table 3). Clearance from the urine was rapid with a half-life ($T_{1/2}$) of 1.9 h and a clearance rate of 54.4 ml/hr/kg (Table 3). At 8 h only 12% of the Cmax concentration remained in the urine. Distribution to the feces was slower compared to the urine with the Cmax (22.1 μg/gm) occurring 8 h post dose administration. Elimination through the feces was also slower with a $T_{1/2}$ of 21 h and a clearance rate of 25.8 g/hr/kg. At 24 h post dose 49% of the Cmax concentration remained in the feces. These results indicate, clearance through the

urine is the primary route of elimination for the SiNPs. It is unlikely that elimination of SiNP via the urine is a result of glomular filtration since the effective pore size of the glomerular wall is only 8 nm and the diameter of the SiNPs used in this study was 33 nm. It is most likely that the SiNPS were secreted into the urine by the mechanism of tubular secretion. The particles would have been secreted from the plasma directly through the epithelial cells lining the renal tubules into the tubular fluid. The endothelial cells contain fenestrations (pores) that are 70 to 90 nm in diameter, thus the 33 nm SiNPs could easily pass though the cells into the tubular fluid and be excreted.

Excretion by way of the fecal route goes through the liver and bile. It is well known that the liver has a high capacity to metabolize xenobiotics. The binding of proteins plays a key role in delivering xenobiotics from the plasma to the liver [30]. In addition the reticuloendothelial system can phagocytize particles then transport them to the liver, which can then be translocated to the bile and excreted in the feces. Chen *et al*. showed that when silica coated quantum dots, had protein bound to their surface *in vivo*, or when they were aggregated to larger particles biliary excretion was favored, and when the particles maintained their original nanosize without *in vivo* protein binding they were rapidly excreted via the kidney [31]. The finding from this current study, showing the presence of a significant amount of SiNPs in the feces is consistent with the particles having protein bound to them and/or being phagocytized into the liver. The aggregation of the particles could further lead to accumulation in the liver for which excretion would favor the biliary route.

CONCLUSIONS

This study was the first to use AMS to comprehensively quantify and track the biological fate of SiNPs over an 8-week exposure period, and was the first to report both the PK and biodistribution of SiNPs *in vivo*. The *in vivo* biodistribution and PK parameters are important aspects for assessing the biosafety of nanomaterials. The biodistribution and PK profiles of nanomaterials are of essential significance for the investigation of tissue/organ toxicity, passive target capacities and biomedical

applications [20]. However, because of their small size it is very difficult to detect and track nanoparticles *in vivo*. Most studies that have investigated the *in vivo* biodistribution of SiNPs have been qualitative in nature [19, 20, 32]. There are very few quantitative biodistribution studies and even fewer that assess the long-term kinetics of SiNPs *in vivo* [9]. Results from this current study show that SiNPs were rapidly distributed to tissues of the reticuloendothelial system and persisted in the tissue over the 8-week time course of the study. Excretion of SiNPs occurred by both the renal and biliary routes. The advantages of using AMS to determine the PK, biodistribution, and excretion characteristics on the SiNPs include the ability to determine long-term kinetics months after administration of SiNPS. Such a complete investigation would not be possible using other methods that lack the necessary sensitivity to detect compounds months after dosing. Detailed pharmacokinetic data require frequent sampling, which is also made possible with AMS detection, by virtue of the small sample sizes needed for analysis. Because of the high sensitivity and small sample size requirement, lower specific activity and less isotope was required for analysis which allowed for studies to be done at radiological doses that would not perturb the natural physiological state of the organism. In addition, the use of AMS allows for future studies to be done at exposures that are environmentally or therapeutically relevant which makes it amenable to human tracer studies.

EXPERIMENTAL SECTION

Materials. ^{14}C-Labeled 33 nm silica dioxide nanoparticles (specific activity 0.23 nCi/mg) and unlabeled nanoparticles were provided by Oak Ridge National Laboratory, Oak Ridge, TN. Sodium heparin, type IV, collagenase and DNAase 1 was purchased from Sigma-Aldrich Inc. (St. Louis MO). Universol scintillation cocktail was obtained by MP Biomedicals (Solon, OH). All other reagents were of analytical grade or better.

Nanoparticle Synthesis and Stability. The synthesis of the ^{14}C-labeled and unlabeled SiNPs, and the biological stability will be reported elsewhere (in preparation). Briefly, SiO_2 particles were produced by hydrolyzing

tetraethoxysilane with NH_3 as a catalyst in microemulsion media[333332] based on the Stöber method [34]. To introduce the ^{14}C isotope into SiO_2, ^{14}C-acrylic acid was used as a ^{14}C precursor. The ^{14}C-acrylic acid (2.5mg, 62.5μCi) and 0.46g allyltrimethoxysilane was first added into the microemulsion under magnetic stirring, and then 0.2mL of saturated $(NH_4)_2S_2O_8$ solution was added. With $(NH_4)_2S_2O_8$ as initiator, the ^{14}C was chemically grafted into a silane agent through radical induced polymerization between the ^{14}C-acrylic acid and allyltrimethoxysilane.

Biological stability of the ^{14}C-SiNPs was evaluated in saline and fetal bovine serum (FBS, Gibco, Invitrogen) over 8 weeks. No significant loss of ^{14}C- label was observed for either solution, indicating that the labeled particles remained intact over the study period.

Animals. Animal experiments were conducted following all the guidelines and regulations set by Lawrence Livermore National Laboratory and with IACUC approval. Six to eight week old male BALB/c mice weighing 25-30 g, with a surgically implanted jugular vein catheter, were obtained from Jackson Labs (Bar Harbor, ME). Animals were housed individually in polystyrene cages containing hardwood bedding and kept on a 12 h light/dark cycle in a ventilated room maintained at 24°C in an AAALAC accredited facility. Animals were provided food (standard lab chow) and water *ad libitum*.

SiNP Biodistribution studies. Mice (n=5) were administered a single intravenous dose of 0.5 mg ^{14}C-SiO_2 nanoparticles (specific activity 0.23 nCi/mg) in 50 μl saline through an implanted jugular vein catheter. The nanoparticle injection was immediately followed by an injection of 50 μl of saline into the catheter to ensure complete infusion of the nanoparticle solution into the blood stream. At designated time points up through eight weeks (see results for time points) animals were euthanized by CO_2 asphyxiation. A subset of animals was placed in metabolism cages and urine and feces were collected over the first 24 h after ^{14}C-SiNP administration. Following euthanasia and subsequent open thoracotomy, blood was collected via cardiac puncture, and tissues were harvested. Whole blood was placed into Microtainer® tubes coated with lithium heparin (Bectin Dickinson,

Franklin Lakes, NJ) and placed on ice. Plasma was separated from the whole blood by centrifugation (10,000 x g for 2 min) within 1 hour of collection, the volume recorded and stored at -80°C until analysis. Tissues were excised from the carcass, rinsed twice in phosphate buffered saline (PBS), placed in pre-weighed glass vials (28 x 60 mm), and immediately frozen at -20° C until analysis. Clean unused surgical tools were used for each animal to avoid cross contamination of radiocarbon. Tissues collected included liver, spleen, kidney, lung, heart, bone marrow, upper gi, colon, muscle, adipose, brain, and cervical lymph nodes.

Preparation of samples for AMS analysis. To ensure a uniform sampling distribution of nanoparticles within each tissue, a tissue digestion procedure was developed that provided a homogenous solution of tissue that was compatible with AMS analysis. Tissues were incubated in 1-2 ml of a 0.11 M KCl based buffer, containing 3.4 mM NaCl , 0.4 mM $MgSO_4$, 40 mM $CaCl_2$, 4 mg/ml type IV collagenase, and 1.1 U/ml DNAse 1. Samples were incubated overnight at 37°C in a shaking water bath with gentle agitation. After the incubation time, samples were vortexed vigorously for 1-3 min to break up any solid particles to ensure complete digestion of the tissues. Plasma and urine samples were analyzed neat without any treatment.

Preparation of the samples for radiocarbon analysis by AMS requires conversion of the samples to graphite. This procedure has been described previously [35]. Briefly, all the tissues and reagents were handled carefully to avoid radiocarbon cross-contamination. This required using disposable materials for any item that might come into contact with the samples. A 30-50 µl aliquot of each tissue homogenate was pipetted into 6 X 55 mm quartz tubes using aerosol resistant tips. For small samples such as bone marrow and lymph tissue, 1 mg of carbon in the form of tributyrin (carrier carbon) was added to the samples to bring the total carbon content to 1 mg (this provided the optimal amount of carbon for efficient conversion to graphite). All samples were subsequently dried under vacuum centrifugation. The dried samples were then converted to graphite by a two-step process using reported methods [36]. Briefly, the dried samples were oxidized to CO_2 by heating at 900° C for 4 h in the presence of copper oxide. The CO_2 was then

cryogenically transferred to a septa-sealed vial under vacuum and reduced to filamentous graphite in the presence of cobalt, titanium hydride, and zinc powder.

AMS Analysis. The radiocarbon content of the tissue homogenate, plasma, and excreta were determined by AMS as described previously [36-38]. The $^{14}C/^{12}C$ ratios from the graphitized samples obtained by AMS were converted to μg SiNPs per mg tissue or ml of plasma/urine after subtraction of the background carbon contributed from the sample and carrier carbon, and correction for the specific activity of the ^{14}C-SiNPs, and the carbon content of the sample [23]. The carbon content of each tissue was determined using a CE-440 elemental analyzer (Exeter Analytical, Inc. North Chelmsford, MA). Tissues were determined to have a carbon content ranging between 10%-15%. Plasma carbon content was 3.8% and urine carbon content was variable between 0.5%-3%.

Pharmacokinetic analysis. Pharmacokinetic parameters of SiNPs in plasma urine and feces were determined by non-compartmental analysis. Concentration of SiNPs over time was determined by quantifying the amount of ^{14}C-SiNP equivalents at each time point and constructing concentration vs. time curves. Solutions Software (Summit Research Services, Montrose, CO) was used to perform noncompartmental analysis of the data for determination of the kinetic parameters for SiNPS. The half life ($T_{1/2}$) and initial SiNP concentration ($C_{initial}$) were determined by observations from the concentration versus time data. Area under the curve (AUC) was calculated for intervals 0 to *t* and 0 to ∞ where *t* is the time of the last measurable concentration (48 h) and ∞ is infinity, using the linear trapezoidal method. Volume of distribution (Vd) was determined based on the AUC determination and reflects the Vd during the elimination phase. The Clearance calculation is based on the $AUC_{0-\infty}$ and assumes 100% bioavailability. Additionally, to estimate the absorption and disposition rate constants, a two-compartment open model was fit to the plasma concentration time profile. Estimated parameters include the absorption rate of SiNPs to the peripheral compartment from the central compartment (K_{12}), the transfer rate of SiNPs from the peripheral compartment to the central compartment (k_{21}), and the elimination rate constant (k_{10}).

ACKNOWLEDGEMENTS

This work was performed under the auspices of the U.S. Department of Energy by, Lawrence Livermore National Laboratory at the Research Resource for Biomedical AMS under contract DE-AC52-07NA27344, and supported by grants from the National Center for Research Resources (5P41RR013461-14) and the National Institute of General Medical Sciences (8 P41 GM103483-14) from the National Institutes of Health, and by Battelle Memorial Institute, CRADA No. PNNL/284.

REFERENCES

1. Yang, J.; Lee, J.; Kang, J.; Lee, K.; Suh, J. S.; Yoon, H. G.; Huh, Y. M.; Haam, S., Hollow silica nanocontainers as drug delivery vehicles. *Langmuir* **2008,** *24* (7), 3417-21.
2. Iezzi, E. B.; Duchamp, J. C.; Harich, K.; Glass, T. E.; Lee, H. M.; Olmstead, M. M.; Balch, A. L.; Dorn, H. C., A symmetric derivative of the trimetallic nitride endohedral metallofullerene, Sc3N@C80. *J Am Chem Soc* **2002,** *124* (4), 524-5.
3. Zhao, X.; Hilliard, L. R.; Mechery, S. J.; Wang, Y.; Bagwe, R. P.; Jin, S.; Tan, W., A rapid bioassay for single bacterial cell quantitation using bioconjugated nanoparticles. *Proc Natl Acad Sci U S A* **2004,** *101* (42), 15027-32.
4. Hirsch, L. R.; Stafford, R. J.; Bankson, J. A.; Sershen, S. R.; Rivera, B.; Price, R. E.; Hazle, J. D.; Halas, N. J.; West, J. L., Nanoshell-mediated near-infrared thermal therapy of tumors under magnetic resonance guidance. *Proc Natl Acad Sci U S A* **2003,** *100* (23), 13549-54.
5. Huo, Q. S.; Liu, J.; Wang, L. Q.; Jiang, Y. B.; Lambert, T. N.; Fang, E., A new class of silica cross-linked micellar core-shell nanoparticles. *Journal of the American Chemical Society* **2006,** *128*, 6447-6453.
6. Roy, I.; Ohulchanskyy, T. Y.; Bharali, D. J.; Pudavar, H. E.; Mistretta, R. A.; Kaur, N.; Prasad, P. N., Optical tracking of organically modified silica nanoparticles as DNA carriers: a nonviral, nanomedicine approach for gene delivery. *Proc Natl Acad Sci U S A* **2005,** *102* (2), 279-84.
7. Slowing, II; Trewyn, B. G.; Lin, V. S., Mesoporous silica nanoparticles for intracellular delivery of membrane-impermeable proteins. *J Am Chem Soc* **2007,** *129* (28), 8845-9.
8. Lin, W.; Huang, Y. W.; Zhou, X. D.; Ma, Y., In vitro toxicity of silica nanoparticles in human lung cancer cells. *Toxicol Appl Pharmacol* **2006,** *217* (3), 252-9.
9. Xie, G.; Sun, J.; Zhong, G.; Shi, L.; Zhang, D., Biodistribution and toxicity of intravenously administered silica nanoparticles in mice. *Arch Toxicol* **2010,** *84* (3), 183-90.
10. Fischer, H. C.; Chan, W. C., Nanotoxicity: the growing need for in vivo study. *Curr Opin Biotechnol* **2007,** *18* (6), 565-71.
11. Colvin, V. L., The potential environmental impact of engineered nanomaterials. *Nat Biotechnol* **2003,** *21* (10), 1166-70.
12. Saffiotti, U., Lung cancer induction by crystalline silica. *Prog Clin Biol Res* **1992,** *374*, 51-69.
13. Kirchner, C.; Liedl, T.; Kudera, S.; Pellegrino, T.; Munoz Javier, A.; Gaub, H. E.; Stolzle, S.; Fertig, N.; Parak, W. J., Cytotoxicity of colloidal CdSe and CdSe/ZnS nanoparticles. *Nano Lett* **2005,** *5* (2), 331-8.
14. Choi, H. S.; Liu, W.; Misra, P.; Tanaka, E.; Zimmer, J. P.; Itty Ipe, B.; Bawendi, M. G.; Frangioni, J. V., Renal clearance of quantum dots. *Nat Biotechnol* **2007,** *25* (10), 1165-70.
15. Kamps, J. A.; Morselt, H. W.; Swart, P. J.; Meijer, D. K.; Scherphof, G. L., Massive targeting of liposomes, surface-modified with anionized albumins, to hepatic endothelial cells. *Proc Natl Acad Sci U S A* **1997,** *94* (21), 11681-5.

16. Krieger, M.; Herz, J., Structures and functions of multiligand lipoprotein receptors: macrophage scavenger receptors and LDL receptor-related protein (LRP). *Annu Rev Biochem* **1994,** *63*, 601-37.
17. Liu, Z.; Cai, W.; He, L.; Nakayama, N.; Chen, K.; Sun, X.; Chen, X.; Dai, H., In vivo biodistribution and highly efficient tumour targeting of carbon nanotubes in mice. *Nat Nanotechnol* **2007,** *2* (1), 47-52.
18. Singh, R.; Pantarotto, D.; Lacerda, L.; Pastorin, G.; Klumpp, C.; Prato, M.; Bianco, A.; Kostarelos, K., Tissue biodistribution and blood clearance rates of intravenously administered carbon nanotube radiotracers. *Proc Natl Acad Sci U S A* **2006,** *103* (9), 3357-62.
19. Cho, M.; Cho, W. S.; Choi, M.; Kim, S. J.; Han, B. S.; Kim, S. H.; Kim, H. O.; Sheen, Y. Y.; Jeong, J., The impact of size on tissue distribution and elimination by single intravenous injection of silica nanoparticles. *Toxicol Lett* **2009,** *189* (3), 177-83.
20. He, Q.; Zhang, Z.; Gao, F.; Li, Y.; Shi, J., In vivo biodistribution and urinary excretion of mesoporous silica nanoparticles: effects of particle size and PEGylation. *Small* **2011,** *7* (2), 271-80.
21. Liu, T.; Li, L.; Teng, X.; Huang, X.; Liu, H.; Chen, D.; Ren, J.; He, J.; Tang, F., Single and repeated dose toxicity of mesoporous hollow silica nanoparticles in intravenously exposed mice. *Biomaterials* **2011,** *32*, 1657-1668.
22. He, X.; Nie, H.; Wang, K.; Tan, W.; Wu, X.; Zhang, P., In vivo study of biodistribution and urinary excretion of surface-modified silica nanoparticles. *Anal Chem* **2008,** *80* (24), 9597-603.
23. Vogel, J. S.; Turteltaub, K. W.; Finkel, R. C.; Nelson, D. E., Accelerator mass spectrometry — isotope quantification at attomole sensitivity. *Anal. Chem.* **1995,** *67*, A353-A359.
24. Lappin, G.; Garner, R. C., Current perspectives of 14C-isotope measurement in biomedical accelerator mass spectrometry. *Anal Bioanal Chem* **2004,** *378* (2), 356-64.
25. Turteltaub, K. W.; Watkins, B. E.; Vanderlaan, M.; Felton, J. S., Role of metabolism on the DNA binding of MeIQx in mice and bacteria. *Carcinogenesis* **1990,** *11*, 43-49.
26. Frantz, C. E.; Bangerter, C.; Fultz, E.; Mayer, K. M.; Vogel, J. S.; Turteltaub, K. W., Dose-response studies of MeIQx in rat liver and liver DNA at low doses. *Carcinogenesis* **1995,** *16*, 367-373.
27. Dueker, S. R.; Lin, Y.; Buchholz, B. A.; Schneider, P. D.; Lame, M. W.; Segall, H. J.; Vogel, J. S.; Clifford, A. J., Long-term kinetic study of beta-carotene, using accelerator mass spectrometry in an adult volunteer. *J Lipid Res* **2000,** *41* (11), 1790-800.
28. van Schooneveld, M. M.; Vucic, E.; Koole, R.; Zhou, Y.; Stocks, J.; Cormode, D. P.; Tang, C. Y.; Gordon, R. E.; Nicolay, K.; Meijerink, A.; Fayad, Z. A.; Mulder, W. J., Improved biocompatibility and pharmacokinetics of silica nanoparticles by means of a lipid coating: a multimodality investigation. *Nano Lett* **2008,** *8* (8), 2517-25.
29. Saba, T. M., Physiology and physiopathology of the reticuloendothelial system. *Arch. Intern. Med.* **1970,** *126*, 1031-1052.

30. Levi, A. J.; Gatmaitan, Z.; Arias, I. M., Two hepatic cytoplasmic protein fractions, Y and Z, and their possible role in the hepatic uptake of bilirubin, sulfobromophthalein, and other anions. *J Clin Invest* **1969,** *48* (11), 2156-67.
31. Chen, Z.; Chen, H.; Meng, H.; Xing, G.; Gao, X.; Sun, B.; Shi, X.; Yuan, H.; Zhang, C.; Liu, R.; Zhao, F.; Zhao, Y.; Fang, X., Bio-distribution and metabolic paths of silica coated CdSeS quantum dots. *Toxicol Appl Pharmacol* **2008,** *230* (3), 364-71.
32. Kumar, R.; Roy, I.; Ohulchanskky, T. Y.; Vathy, L. A.; Bergey, E. J.; Sajjad, M.; Prasad, P. N., In vivo biodistribution and clearance studies using multimodal organically modified silica nanoparticles. *ACS Nano* **2010,** *4* (2), 699-708.
33. Wang, W.; Asher, S. A., Photochemical incorporation of silver quantum dots in monodisperse silica colloids for photonic crystal applications. *Journal of the American Chemical Society* **2001,** *123* (50), 12528-12535.
34. Stöber, W.; Fink, A.; Bohn, E., Controlled growth of monodisperse silica spheres in the micron size range. *J. Colloid Interface Sci* **1968,** *26*, 62-69.
35. Creek, M. R.; Mani, C.; Vogel, J. S.; Turteltaub, K. W., Tissue distribution and macromolecular binding of extremely low doses of [14C]-benzene in B6C3F1 mice. *Carcinogenesis* **1997,** *18* (12), 2421-7.
36. Ognibene, T. J.; Bench, G.; Vogel, J. S.; Peaslee, G. F.; Murov, S., A high-throughput method for the conversion of CO2 obtained from biochemical samples to graphite in septa-sealed vials for quantification of 14C via accelerator mass spectrometry. *Anal Chem* **2003,** *75* (9), 2192-6.
37. Turteltaub, K. W.; Felton, J. S.; Gledhill, B. L.; Vogel, J. S.; Southon, J. R.; Caffee, M. W.; Finkel, R. C.; Nelson, D. E.; Proctor, I. D.; Davis, J. C., Accelerator mass spectrometry in biomedical dosimetry: relationship between low-level exposure and covalent binding of heterocyclic amine carcinogens to DNA. *Proc. Natl. Acad. Sci. USA* **1990,** *87*, 5288-5292.
38. Vogel, J. S., Rapid production of graphite without contamination for biomedical AMS. *Radiocarbon* **1992,** *34*, 333-350.

Table 1. Mean plasma pharmacokinetic parameters of SiO_2 nanoparticles following a single intravenous administration of 0.5 mg ^{14}C-SiO_2 nanoparticles to male BALB/c mice

Dose (mg)	$C_{(initial)}$ (μg/mL)	$t_{1/2}\,\alpha$ (hr)	$t_{1/2}\,\beta$ (hr)	$AUC_{0\text{-}t}$ (μg-hr/mL)	$AUC_{0\text{-}\infty}$ (μg-hr/mL)	CL (mL/hr/kg)	V_d (mL/kg)	V_{ss} (ml)	k_{12} (hr^{-1})	k_{21} (hr^{-1})	k_{10} (hr^{-1})
0.5	154.0	0.38	78.4	445.5	1099.4	18.2	2058.1	46.8	1.58	0.11	0.14

Table 2. Mean tissue concentration of ^{14}C-SiNP (33 nm), over time (0-24 h), following single 0.5 mg intravenous administration to male BALB/c mice

	μg SiO_2 nanoparticles/gm tissue ± SEM					
	0.25 hr	0.5 hr	1.0 hr	2.0 hr	8 hr	24 hr
Liver	145.24 ± 22.96	162.43 ± 2.61	157.52 ± 1.41	228.20 ± 7.46	112.81 ± 4.41	74.21 ± 4.58
Spleen	185.14 ± 38.46	195 .07 ± 20.15	202.29 ± 21.30	298.6 5± 43.4	162.15 ± 13.4	85.64 ± 13.33
Kidney	63.07 ± 9.09	45.10 ± 2.56	35.91 ± 8.80	56.91 ± 13.6	25.11 ± 2.39	14.66 ± 1.16
Lung	41.12 ± 4.05	67.22 ± 15.20	45.05 ± 4.43	33.11 ± 9.11	12.12 ± 2.22	9.02 ± 2.59
Heart	17.47 ± 2.60	12.35 ± 1.10	6.43 ± 1.41	13.26 ± 4.46	6.05 ± 0.11	5.31 ± 0.57
Colon	3.43 ± 0.43	2.65 ± 0.89	2.14 ± 0.65	5.44 ± 2.66	1.80 ± 0.25	0.88 ± 0.16
Upper gi	6.04 ± 1.65	5.76 ± 2.42	2.66 ± 0.38	6.56 ± 1.21	5.20 ± 1.89	3.96 ± 3.67
Muscle	1.57 ± 0.34	0.95 ± 0.10	0.53 ± 0.06	1.18 ± 0.51	0.50 ± 0.07	0.47 ± 0.14
Adipose	8.37 ± 1.22	4.64 ± 0.66	3.13 ± 1.02	3.59 ± 0.93	1.22 ± 0.20	0.70 ± 0.34
Brain	1.45 ± 0.39	0.94 ± 0.39	0.53 ± 0.14	0.72 ± 0.37	0.08 ± 0.01	0.03 ± 0.009
Bone marrow	43.99 ± 10.40	6.56 ± 2.24	10.20 ± 5.14	9.38 ± 3.46	4.79 ± 1.25	5.54 ± 2.25
Cervical lymph	14.94 ± 5.62	9.64 ± 1.19	17.43 ± 9.15	33.92 ± 6.62	20.47 ± 10.02	6.08 ± 0.59

Table 2 continued. Mean tissue concentration of ^{14}C-SiNP (33 nm), over time (1-56 days), following single 0.5 mg intravenous administration to male BALB/c mice

	µg SiO_2 nanoparticles/gm tissue ± SEM						
	1 day	2 day	7 days	14 days	28 days	42 days	56 days
Liver	74.21 ± 4.58	106.68 ± 10.3	100.5 ± 4.09	80.23 ± 7.59	55.57 ± 6.26	30.23 ± 3.25	20.99 ± 1.69
Spleen	85.64 ± 13.33	137.88 ± 18.7	143.5 ± 11.75	158.75 ± 6.71	195.61 ± 26.1	78.96 ± 13.64	36.93 ± 2.71
Kidney	14.66 ± 1.16	19.40 ± 3.78	22.7 ± 11.48	13.67 ± 1.57	26.38 ± 4.51	18.1 ± 3.84	12.11 ± 1.81
Lung	9.02 ± 2.59	8.68 ± 0.57	24.33 ± 5.67	18.78 ± 6.95	5.14 ± 1.84	3.09 ± 0.44	7.40 ± 1.48
Heart	5.31 ± 0.57	5.78 ± 0.31	1.27 ± 0.16	0.86 ± 0.11	1.27 ± 0.37	0.68 ± 0.05	0.43 ± 0.03
Colon	0.88 ± 0.16	1.34 ± 0.15	1.01 ± 0.36	0.39 ± 0.11	2.75 ± 1.99	0.94 ± 0.091	0.68 ± 0.12
Upper gi	3.96 ± 3.67	3.43 ± 1.45	1.20 ± 0.15	0.90 ± 0.14	16.27 ± 7.54	6.29 ± 2.04	4.65 ± 1.16
Muscle	0.47 ± 0.14	0.30 ± 0.06	0.38 ± 0.14	0.23 ± 0.05	0.23 ± 0.06	0.16 ± 0.02	0.14 ± 0.01
Adipose	0.70 ± 0.34	1.05 ± 0.33	1.09 ± 0.76	0.22 ± 0.10	1.32 ± 0.18	3.48 ± 0.28	2.93 ± 0.31
Brain	0.03 ± 0.009	0.06 ± 0.003	0.32 ± 0.15	0.07 ± 0.02	0.06 ± 0.01	0.32 ± 0.04	0.29 ± 0.01
Bone marrow	5.54 ± 2.25	11.55 ± 6.31	12.45 ± 2.31	4.41 ± 0.86	0.85 ± 0.14	1.51 ± 0.48	2.17 ± 1.4
Cervical lymph	6.08 ± 0.59	12.05 ± 6.61	6.35 ± 4.15	4.14 ± 1.38	4.42 ± 1.47	1.97 ± 0.54	1.82 ± 0.66

Table 3. Mean (n=5) excretion kinetics of SiO_2 nanoparticles following a single intravenous administration of 0.5 mg ^{14}C-SiO_2 nanoparticles to male BALB/c mice

Elimination route	$C_{(max)}$	$T_{(max)}$ (h)	$t_{1/2}$ (h)	CL (mL/h/kg)
urine	62.4 µg/ml	2.0	1.9	54.4
feces	22.0 µg/gm	8.0	22.1	25.8

Figure Legends

Figure 1. Mean plasma concentration versus time curve of ^{14}C-SiNP (33 nm), following single 0.5 mg intravenous administration to BALB/c male mice. Results are the mean of 5 animals ± the standard error of the mean.

Figure 2. Mean tissue concentration of ^{14}C-SiNP (33 nm), over a 24 h sampling time, following single 0.5 mg intravenous administration to BALB/c male mice. Data is expressed as the mean of 5 animals ± the standard error of the mean.

Figure 3. Mean concentration of ^{14}C-SiNP (33 nm) in urine and feces, over a 24 h sampling time, following single 0.5 mg intravenous administration to BALB/c male mice. Data is expressed as µg of ^{14}C-SiNP/ml of urine and µg of ^{14}C-SiNP/gm of feces. Results are the mean of 5 animals ± the standard error of the mean.

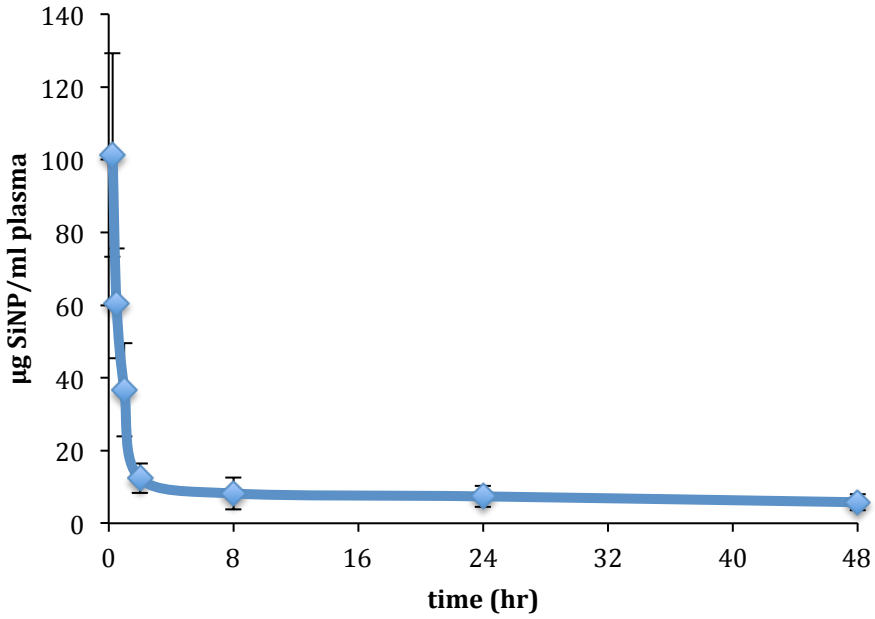
140
120
100
80
60
40
20
0
µg SiNP/ml plasma
0
8
16
24
32
40
48
time (hr)

Figure 1

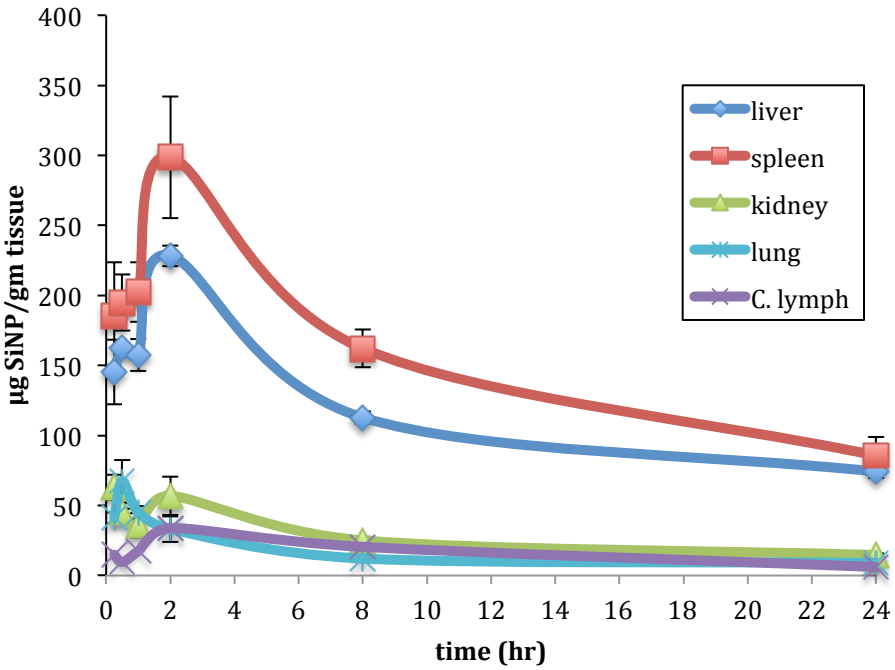
400
350
300
250
200
150
100
50
0
µg SiNP/gm tissue
0
2
4
6
8
10
12
14
16
18
20
22
24
time (hr)
liver
spleen
kidney
lung
C. lymph

Figure 2

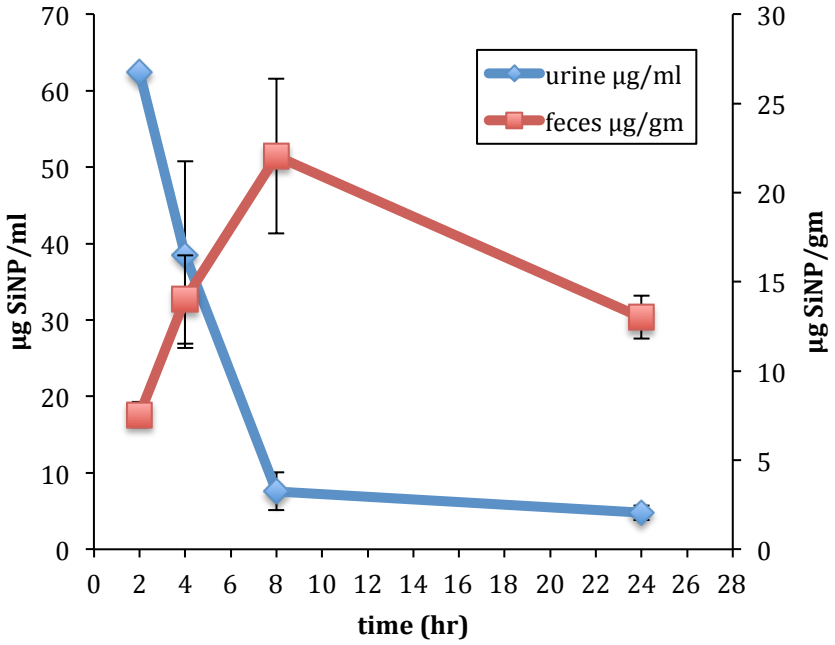
urine µg/ml
feces µg/gm
µg SiNP/ml
µg SiNP/gm
time (hr)
0
10
20
30
40
50
60
70
0
5
10
15
20
25
30
0 2 4 6 8 10 12 14 16 18 20 22 24 26 28

Figure 3